

p-wave Pairing in Two-Component Fermi System with Unequal Population: Weak Coupling BCS to Strong Coupling BEC Regimes

Renyuan Liao, Florentin Popescu, and Khandker Quader
Department of Physics, Kent State University, Kent, OH 44242
 (Dated: October 24, 2012)

We study p -wave pairing in a two-component Fermi system with unequal population across weak-coupling BCS to strong-coupling BEC regimes. We find a rich $m_s = 0$ spin triplet p -wave superfluid ground state structure as a function of population imbalance. Under a phase stability condition, the “global” energy minimum is given by a multitude of “mixed” SF states formed of linear combinations of $m = \pm 1, 0$ sub-states of the $\ell = 1$ orbital angular momentum state. Except for the “pure” SF states, ($\ell = 1, m = \pm 1$), other states exhibit oscillation in energy with the relative phase between the constituent gap amplitudes. We also find states with “local” energy minimum that can be stable at higher polarizations, suggesting a quantum phase transition between the “global” and “local” minima phases driven by polarization. The local and global minimum states may be associated with Morse and non-Morse critical points. We discuss possible consequences for experiments.

PACS numbers: 03.75.Ss, 05.30.Fk, 74.20.Rp, 74.20.De, 67.85.-d, 67.85.Fg, 34.50.-s

Introduction: Over past several years there has been sustained interest in paired fermion ground states with unconventional pairing symmetry. Among these are p -wave spin triplet condensates. Correlated electron systems, such as, SrRu_2O_4 [1] and ferromagnetic superconductors [2] are believed to possess p -wave triplet symmetry. Fermi systems with unequal species population, as quark matter [3], magnetic field induced organic superconductors [4] and cold fermion systems with unequally populated hyperfine states [5], add a fascinating dimension. Discovery of s -wave superfluidity in cold atoms [6] subjected to s -wave Feshbach resonance (FR), and observations of p -wave FR [7–10] in ^6Li and ^{40}K had raised the prospect for observing p -wave superfluidity in cold Fermi gases. While this may be difficult to achieve, alternate methods [11] and optical lattices [12, 13] offer encouraging prospects. There has been theory work on p -wave superfluidity in BEC-BCS crossover region for a single-component Fermi gas [14–17], and two-component case [18] with equal-species population. However, theoretical work on p -wave pairing for unequal population has been limited [13, 19].

In this paper, we conduct analytical and numerical study of p -wave superfluidity in a two-component Fermi system with *unequal* population, across weak-coupling BCS to strong coupling BEC regimes. We consider the case where inter-species pairing interaction is dominant. While this is interesting to study on general grounds, we are also motivated by work [13] on population-imbalanced Fermi mixtures in optical lattices, and the observation [9, 18] that unlike liquid ^3He , pairing interaction in cold atoms may be highly anisotropic in “spin”-space. (“spin” referring to hyperfine states). For example, in ^6Li , when the hyperfine pair $|m_s, m'_s\rangle = |1/2, -1/2\rangle$ is at resonance, the pairs $|1/2, 1/2\rangle$ and $|-1/2, -1/2\rangle$ would not be. So, intra-spin interactions can be neglected. Pairs in p -wave superfluids with

unlike “spin” components can, however, have different $\ell = 1$ components: $m = \pm 1, 0$. Then the gap parameters $\Delta_{\ell=1,m}$ are related to the spherical harmonics, $Y_{1,m=\pm 1,0}$.

Our *key* results are: We find a rich superfluid (SF) ground state (GS) structure. Under a condition on relative phase between pairing amplitudes $\Delta_{m=0,\pm 1}$ ($\Delta_{\ell=1,m} \equiv \Delta_m$), a multitude of “mixed” superfluid states of the form $a_0\Delta_0 + a_1\Delta_1 + a_{-1}\Delta_{-1}$ are found to be degenerate with $\Delta_{\pm 1}$; these give the global minimum GS energy. Additionally, we find states with *local* minimum energy. We provide a geometric representation of the states (Fig. 1). Our $T=0$ polarization (P) vs p -wave coupling phase diagram (Fig. 2) shows two SF phases, comprising respectively of states with global and local minimum energy, and a region of phase separation. This suggests the intriguing possibility of a quantum phase transition between the two SF phases, driven by polarization. The $P \neq 0$ GS structure is preserved in the $P \rightarrow 0$ limit; hence richer than previous $P = 0$ results [18]. The energies of the “mixed” states oscillate with the relative phase angle (Fig.3); this may be interesting to explore experimentally.

Model: We consider a system of fermions with unequal “spin” ($(\uparrow, \downarrow) \equiv (1/2, -1/2)$) population, but with equal mass. Pairing interactions in all $\ell = 1$ channels ($m = 0, \pm 1$) are assumed equal; intra-species interactions ($\uparrow\uparrow$ or $\downarrow\downarrow$) are set to zero. Since we adjust self-consistently the chemical potential with the strength and sign of the coupling, in our fermion-only model, molecules appear naturally as 2-fermion bound states. The $S = 1, m_s = 0$ triplet pairing Hamiltonian is given by:

$$\mathcal{H} = \sum_{\mathbf{k}\sigma} \xi_{\mathbf{k}\sigma} c_{\mathbf{k}\sigma}^\dagger c_{\mathbf{k}\sigma} + \sum_{\mathbf{k}\mathbf{k}'\mathbf{q}} V_{\mathbf{k}\mathbf{k}'} c_{\mathbf{k}+\mathbf{q}/2\uparrow}^\dagger c_{-\mathbf{k}+\mathbf{q}/2\downarrow}^\dagger c_{-\mathbf{k}'+\mathbf{q}/2\downarrow} c_{\mathbf{k}'+\mathbf{q}/2\uparrow} \quad (1)$$

where $c_{\mathbf{k}\sigma}$ ($c_{\mathbf{k}\sigma}^\dagger$) is the annihilation (creation) opera-

tor for a fermion with momentum \mathbf{k} , kinetic energy $\xi_{\mathbf{k}\sigma} = \epsilon_{\mathbf{k}} - \mu_{\sigma}$, spin σ ; μ_{σ} is the species chemical potential, and $\epsilon_{\mathbf{k}} = \hbar^2 k^2 / 2m$. $V_{\mathbf{k}\mathbf{k}'}$ is the pairing interaction.

We consider condensate pairs with zero center-of-mass momentum ($\mathbf{q}=0$). While non-zero \mathbf{q} is interesting from the perspective of FFLO [20] states, the problem of $\mathbf{q} = 0$ unconventional pairing in unequal-population systems is rich in itself. \mathcal{H} is mean-field (MF) decoupled via $S = 1, m_s = 0$ “spin”-triplet pairing gap function $\Delta_{\uparrow\downarrow}(\mathbf{k}) \equiv \Delta(\mathbf{k}) = -\sum_{\mathbf{k}'} V_{\mathbf{k}\mathbf{k}'} \langle c_{-\mathbf{k}'\downarrow} c_{\mathbf{k}'\uparrow} \rangle$ giving:

$$\mathcal{H}^{\text{MF}} = \sum_{\mathbf{k}\sigma} \xi_{\mathbf{k}\sigma} c_{\mathbf{k}\sigma}^\dagger c_{\mathbf{k}\sigma} - \sum_{\mathbf{k}} \left[\Delta(\mathbf{k}) c_{\mathbf{k}\uparrow}^\dagger c_{-\mathbf{k}\downarrow}^\dagger + \text{H.c.} \right] - \sum_{\mathbf{k}, \mathbf{k}'} V_{\mathbf{k}\mathbf{k}'} \langle c_{\mathbf{k}\uparrow}^\dagger c_{-\mathbf{k}\downarrow}^\dagger \rangle \langle c_{-\mathbf{k}'\downarrow} c_{\mathbf{k}'\uparrow} \rangle \quad (2)$$

To obtain GS energy of the MF Hamiltonian (2) we use the equation-of-motion method [21, 22] for the imaginary-time ($\tau = it$) normal ($G_{\sigma\sigma'}$) and anomalous ($F_{\sigma\sigma'}$) Green's functions [23]:

$$\partial_\tau G_{\sigma\sigma'}(\mathbf{k}, \tau) = -\delta(\tau) \delta_{\sigma\sigma'} - \xi_{\mathbf{k}\sigma} G_{\sigma\sigma'}(\mathbf{k}, \tau) + \Delta_{-\sigma\sigma}(\mathbf{k}) F_{-\sigma\sigma'}(\mathbf{k}, \tau), \quad (3)$$

$$\partial_\tau F_{\sigma\sigma'}(\mathbf{k}, \tau) = \xi_{-\mathbf{k}\sigma} F_{\sigma\sigma'}(\mathbf{k}, \tau) + \Delta_{-\sigma-\sigma}^*(\mathbf{k}) G_{-\sigma\sigma'}(\mathbf{k}, \tau). \quad (4)$$

Eqs. (3) and (4) are Fourier transformed with $\tau \rightarrow i\omega_n \equiv \nu$ and $\partial_\tau \rightarrow -\nu$, where $i\omega_n = (2n+1)\pi T$ are Matsubara frequencies. This gives $G_{\sigma\sigma}(\mathbf{k}, \nu) = -(\xi_{-\mathbf{k}-\sigma} + \nu) / [(\xi_{\mathbf{k}\sigma} - \nu)(\xi_{-\mathbf{k}-\sigma} + \nu) + |\Delta_{\sigma-\sigma}(\mathbf{k})|^2]$, and $F_{\sigma-\sigma}(\mathbf{k}, \nu) = \Delta_{\sigma-\sigma}^*(\mathbf{k}) / [(\xi_{\mathbf{k}\sigma} - \nu)(\xi_{-\mathbf{k}-\sigma} + \nu) + |\Delta_{\sigma-\sigma}(\mathbf{k})|^2] = -F_{-\sigma\sigma}(\mathbf{k}, \nu)$.

In terms of radial and angular parts, $V_{\mathbf{k}\mathbf{k}'} = (4\pi/3) \sum_m V_{kk'} Y_{1,m}(\hat{\mathbf{k}}) Y_{1,m}^*(\hat{\mathbf{k}}')$ ($\hat{\mathbf{k}} = (\theta, \phi)$). Using $\langle c_{-\mathbf{k}'\downarrow} c_{\mathbf{k}'\uparrow} \rangle \equiv F_{\uparrow\downarrow}^*(\mathbf{k}', \tau=0^-)$ and Fourier transforming, we obtain, $\Delta(\mathbf{k}) = -(1/k_B T) \sum_{\nu \mathbf{k}'} V_{\mathbf{k}\mathbf{k}'} F_{\uparrow\downarrow}^*(\mathbf{k}', \nu) e^{\nu 0^+}$. We take $V_{kk'} = \lambda w(k) w(k')$, a separable form chosen for convenience [16, 18, 24]; this does not change physics qualitatively. Then the gap function: $\Delta(\mathbf{k}) = \sum_m \Delta_m w(k) Y_{1,m}(\hat{\mathbf{k}}) \equiv w(k) \Delta(\hat{\mathbf{k}})$, where $\Delta_m = -(1/k_B T) \sum_{\nu \mathbf{k}'} \lambda w(k') Y_{1,m}^*(\hat{\mathbf{k}}') F_{\uparrow\downarrow}^*(k', \nu) e^{\nu 0^+}$. Obtaining $F_{\uparrow\downarrow}(k, \nu)$ and $G_{\sigma\sigma}$ from Eqs. (3)-(4), we get for the $\ell = 1; m = 0, \pm 1$ gap amplitudes,

$$\Delta_m = -\lambda \sum_{\mathbf{k}} w(k) Y_{1,m}^*(\hat{\mathbf{k}}) \Delta(\mathbf{k}) [n_F(E_k^-) - n_F(E_k^+)] / (2E_k) \quad (5)$$

and for the particle number densities,

$$n_\sigma = \sum_{\mathbf{k}} \langle c_{\mathbf{k}\sigma}^\dagger c_{\mathbf{k}\sigma} \rangle = \sum_{\mathbf{k}} G_{\sigma\sigma}(k, \tau = 0^-). \quad (6)$$

Above, $h = (\xi_{k\downarrow} - \xi_{k\uparrow})/2 = (\mu_\uparrow - \mu_\downarrow)/2$, $E_k = [\xi_k^2 + |\Delta^2(\mathbf{k})|]^{1/2}$, with $\xi_k = (\xi_{k\uparrow} + \xi_{k\downarrow})/2 = \epsilon_k - \mu$ and $\mu = (\mu_\uparrow + \mu_\downarrow)/2$; $n_F(E_k^\pm)$ are Fermi functions with $E_k^\pm =$

$-h \pm E_k$. At $T=0$ and for $h>0$, the expectation value of the grand canonical potential is given by:

$$E_g \equiv \langle \mathcal{H} \rangle = \sum_{\mathbf{k}} \left\{ \xi_k - E_k + \frac{|\Delta(\mathbf{k})|^2}{2\epsilon_k} \right\} + \sum_{\mathbf{k}} \{ (E_k - h) \theta(-E_k + h) \} - \frac{1}{g} \sum_m |\Delta_m|^2 \quad (7)$$

Following standard practice, coupling λ has been expressed in terms of the “regularized” interaction g : $1/g = 1/\lambda + (1/(2\pi\hbar)^3) \int w^2(k) d^3\mathbf{k} / 2\epsilon_k$ [25]. For $w(k)$, we adopt the N-SR form [24]: $w(k) = k_0 k / (k_0^2 + k^2)$.

Ground State Analysis: We assume $0 \leq |\Delta(\mathbf{k})| \ll \xi_k$, and expand E_k in Eq.(7) in powers of $|\Delta(\mathbf{k})|$ to 4th order: $E_k \sim |\xi_k| [1 + |\Delta(\mathbf{k})|^2 / 2|\xi_k|^2 - |\Delta(\mathbf{k})|^4 / 8|\xi_k|^4]$. Since $\xi_k \gg |\Delta(\mathbf{k})|$, $\xi_k = 0$ ($\epsilon_k = \mu$) is excluded from the expansion [26]. Substituting this in Eq.(7) and converting momentum sums to integrals we obtain: $E_g = \alpha \int |\Delta(\hat{\mathbf{k}})|^2 d\Omega + \beta \int |\Delta(\hat{\mathbf{k}})|^4 d\Omega + \gamma$, where $\alpha = (1/(2\pi\hbar)^3) \int_{E_k < h} w^2(k) k^2 dk / 2\epsilon_k + (1/(2\pi\hbar)^3) \int_{E_k > h} w^2(k) k^2 dk (1/2\epsilon_k - 1/2|\xi_k|) - 1/g$, $\beta = (1/(2\pi\hbar)^3) \int_{E_k > h} w^4(k) k^2 dk / 8|\xi_k|^3$ and $\gamma = (4\pi/(2\pi\hbar)^3) \int_{E_k < h} (\xi_k - h) k^2 dk$. Existence of a superfluid phase requires $\alpha < 0$, otherwise minimization of E_g forces the gap to vanish. The polarization-dependence ($P = (n_\uparrow - n_\downarrow) / (n_\uparrow + n_\downarrow)$) of E_g is contained in α, β, γ , which depend on h, μ and $w(k)$; α alone depends explicitly on coupling g . Accordingly, the Δ_m 's depend on P .

For fixed (μ, h) , and E_k to $\mathcal{O}(\Delta(\mathbf{k})^4)$, we obtain an analytic expression for the ground state energy, E_G , in terms of the pairing amplitudes Δ_m :

$$E_G = -\frac{\alpha^2}{8\beta} + \gamma + 2\beta \left(|\Delta_0|^2 + |\Delta_1|^2 + |\Delta_{-1}|^2 + \frac{\alpha}{4\beta} \right)^2 + \beta (|\Delta_0|^2 - 2|\Delta_1||\Delta_{-1}|)^2 + 4\beta(1-t)|\Delta_0|^2 |\Delta_1| |\Delta_{-1}| \quad (8)$$

where $t = \cos \theta$, with $\theta = \angle(\Delta_0^*, \Delta_0^* \Delta_{-1}) = 2\phi_0 - \phi_1 - \phi_{-1}$; ϕ_m 's are phases associated with the gap amplitudes Δ_m . Minimizing E_G in (8) with respect to Δ_m 's, we find that for a stable p-wave superfluid phase to exist, the following conditions have to be satisfied simultaneously:

- (a) $|\Delta_0|^2 + |\Delta_1|^2 + |\Delta_{-1}|^2 = -\alpha/4\beta \equiv R^2$ (sphere)
- (b) $|\Delta_0|^2 - 2|\Delta_1||\Delta_{-1}| = 0$ (plane)
- (c) $(1-t)|\Delta_0|^2 |\Delta_1| |\Delta_{-1}| = 0$

For all three Δ_m 's non-zero, conditions (a) and (b) give a semicircle formed by the intersection of the surface of a sphere of radius R , ($R^2 = -\alpha/4\beta$) in $\Delta_1, \Delta_{-1}, \Delta_0$ space, with a plane defined by $|\Delta_1| + |\Delta_{-1}| = R$. Points spanning the semicircle represent a multitude of “mixed” superfluid states of the form $a_0 \Delta_0 + a_1 \Delta_1 + a_{-1} \Delta_{-1}$; a_0, a_1, a_{-1} being constants. A 3D geometric representation of the states is shown in Fig.1. Condition (c)

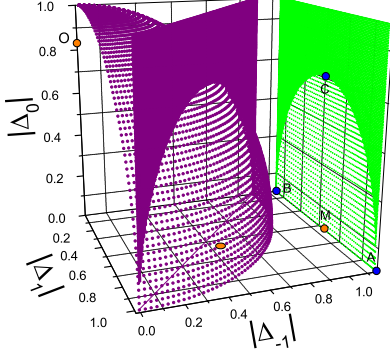


FIG. 1: (Color online) Geometric representation of p-wave states. Semicircle formed by intersection of sphere surface with plane represent a continuum of states exhibiting global energy minimum (see text). Plane containing semicircle is also shown (green). O (on Δ_0 axis) and M (in Δ_1 - Δ_{-1} plane) are states with local energy minimum. Δ_m ($m = 0, \pm 1$)'s normalized to sphere radius $\sqrt{-\alpha/4\beta}$; $\alpha < 0$.

imposes the constraint, $t \equiv \cos \theta = 1$, i.e. the relative phase $\theta = (\phi_0 - \phi_1) - (\phi_{-1} - \phi_0) = 2n\pi$. $t=1$ corresponds to a parallel orientation of vectors $\Delta_0 \Delta_1^*$ and $\Delta_0^* \Delta_{-1}$. The ground state (GS) *global minimum* energy,

$$E_G^{gl} = -\alpha^2/8\beta + \gamma, \quad (\alpha < 0), \quad (10)$$

is completely determined by α, β, γ given earlier.

The phase condition (c) is always satisfied for the states, $\Delta_{\pm 1}$, at the endpoints A, B of the semicircle. But, energies of other states on the semicircle oscillate with θ , and attains E_G^{gl} only for $t = 1$, i.e. $\theta = 2n\pi$ (Fig. 3a). The oscillation amplitudes depends on the specific state; state C at the top of the projected figure (Fig. 1) has the maximum amplitude. Representative states A, B, C on semicircle are given by: (A) $|\Delta_0| = |\Delta_{-1}| = 0$ and $|\Delta_1|^2 = -\alpha/4\beta$; (B) $|\Delta_0| = |\Delta_1| = 0$ and $|\Delta_{-1}|^2 = -\alpha/4\beta$; (C) $|\Delta_0|^2 = -\alpha/8\beta$ and $|\Delta_1|^2 = |\Delta_{-1}|^2 = -\alpha/16\beta$.

We obtain *other* minimum energy solutions by considering special cases in Eq. 8. (i) $|\Delta_1| = 0 = |\Delta_{-1}|$, $|\Delta_0| \neq 0$: we find a unique solution, $|\Delta_0|^2 = -\alpha/6\beta$; point O in Fig. 1. (ii) $|\Delta_0| = 0$: this gives equations for two ellipses in $\Delta_1 - \Delta_{-1}$ plane:

$$\begin{aligned} |\Delta_1|^2 + 2|\Delta_{-1}|^2 + \frac{\alpha}{4\beta} &= 0 \quad (\text{ellipse1}) \\ 2|\Delta_1|^2 + |\Delta_{-1}|^2 + \frac{\alpha}{4\beta} &= 0 \quad (\text{ellipse2}) \end{aligned} \quad (11)$$

Intersection of the two ellipses gives the solution: $|\Delta_1|^2 = |\Delta_{-1}|^2 = -\alpha/12\beta$, $|\Delta_0| = 0$; point M in Fig. 1. Like A and B, states O and M automatically satisfy phase constraint (Eq. 9(c)). These exhaust all possible independent solutions. Incidentally, states A (B) respectively

lie at the intersection of ellipse 1 (ellipse 2), and sphere and plane of Fig. 1. The energies for O and M are equal, and lie higher than E_G^{gl} ; we denote this as *local* minimum energy:

$$E_G^{loc} = -\alpha^2/12\beta + \gamma \quad (\alpha < 0) \quad (12)$$

We checked the stability of the states by examining the stability matrix or Hessian, $H: (\partial^2 E_G / \partial \Delta_{m_i} \partial \Delta_{m_j})$. $\det[H] = 0$ for states A, B, and $\det[H] > 0$ for states O, M; in the language of Catastrophe Theory [27], A, B can be identified with non-Morse "critical" points, and O, M with Morse "critical" points [28].

As can be seen from the expression for γ , and the definition of μ, h , in the limit of zero polarization ($P \rightarrow 0$), the GS energy coefficient $\gamma \rightarrow 0$, while $\alpha < 0, \beta > 0$ attain different numerical values. Accordingly, expressions for E_G^{gl} and E_G^{loc} remain essentially the same for $P \rightarrow 0$, but with different numerical values. States A and B (equivalent to A by symmetry) correspond to the finding of Ref. [18] for $P = 0$.

Numerical Calculations: Detailed numerical study of the p-wave superfluid states confirms our analytical results, and reveals additional features. We solve self-consistently three gap equations (Eq. (5)) and two number equations (Eq. (6)), for fixed population imbalance $P = (n_\uparrow - n_\downarrow)/(n_\uparrow + n_\downarrow)$, and p-wave coupling parameter g . (g is related to the triplet scattering parameter: $g = 25k_F^3 a_t / 8\pi$ for a cutoff $k_0 = 10k_F$). This gives us the gap amplitudes Δ_m , and the chemical potentials μ_σ for different P and $1/k_F^3 a_t$. Using these, we obtain the GS energy E_g from Eq. (7), and the coefficients α, β, γ that determine E_g ; agreement between our numerical and analytical results for E_g is good. We note that fixed $(P, n = n_\uparrow + n_\downarrow)$ is equivalent to fixed (μ, h) used in analytic study above.

To check for *stability* of the p-wave states obtained from numerical solutions, we enforce that the stability matrix $(\partial^2 E_G / \partial \Delta_{m_i} \partial \Delta_{m_j})$ is positive definite; and $\delta p / \delta h > 0$. Based on this, we construct [29] a polarization (P) - coupling ($1/k_F^3 a_t$) *phase diagram*, Fig. 2, in BEC-BCS regimes. SF1 denotes a stable superfluid phase, corresponding to the states on the 'semicircle' (Fig. 1) that give GS *global* minimum, E_G^{gl} . With increased P , polarization-dependent parameters, α, β, γ , that determine E_G^{gl} and E_G^{loc} , change so that the superfluid phase SF2, corresponding to states with *local* minimum, attain energy lower than that of SF1, and hence becomes stable. This suggests the interesting possibility that at $T=0$, polarization may drive a quantum phase transition from SF1 to SF2. It may also be possible to access SF2 at $T \neq 0$. At even larger polarizations, SF2 becomes unstable to phase separation (PS). SF1, SF2, and PS occupy a relatively much narrower part of the phase diagram on the BCS side compared to the BEC side. In our two-component system with inter-species interaction, PS persists into full polarization, $P=1$. This is because at

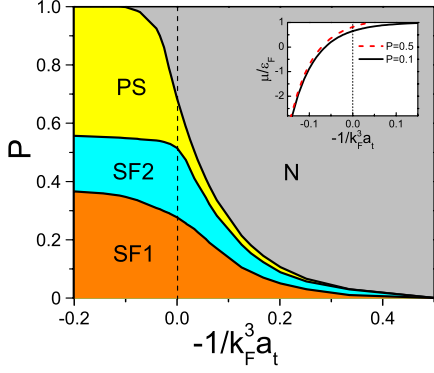


FIG. 2: (Color online) Polarization P vs p-wave coupling $-1/(k_F^3 a_t)$ phase diagram, showing normal (N), p-wave superfluid phases (SF1; SF2), phase separation (PS). Unitarity limit is shown by the dashed vertical line. Inset: Calculated chemical potential vs coupling across BCS/BEC regimes for $P = 0.1$ (solid line), 0.5 (dashed line). Fermi energy, ϵ_F , is given by $\mu/\epsilon_F = 1$ line.

$P=1$, the system is essentially a one-component system; absence of minority-species fermions makes inter-species interaction inoperative. Such a system can exhibit superfluidity only with intra-species interactions.

The inset in Fig. 2 shows the calculated behavior of chemical potential μ across BEC-BCS regimes. It deviates significantly from the Fermi energy ($\mu/\epsilon_F = 1$ line) in a wider region around the BEC-BCS crossover, even on the BCS side, and drops much more rapidly to negative values on the BEC side compared to the s-wave case. For sufficiently weak coupling (BCS regime), $\mu \rightarrow \epsilon_F$.

Except for A, B, the continuum of “mixed” SF states on the semicircle (Fig.1) are characterized by relative phase $2n\pi \leq \theta \leq (2n+2)\pi$, so that their energies oscillate with θ . Numerical results for three cases are shown in Fig 3(a). For $\theta \neq 2n\pi$, energies lie higher than the GS global minimum; maximum amplitude occurring for state C in Fig.1. This raises the possibility of observing θ -oscillation in the states on the semicircle using phase sensitive experimental technique(s). They could also be accessed at finite-T. Figs. 3b, 3c respectively show the variation of E_g with coupling g at fixed polarizations P , and with P for fixed g . E_g is normalized to the Fermi energy $\epsilon_F = \hbar^2 k_F^2 / 2m$, with $2k_F^3 = k_{F\uparrow}^3 + k_{F\downarrow}^3$. For a given P , E_g becomes less negative as g approaches unitarity; the trend is more noticeable for smaller P 's. The energy curves in Fig. 3(b) would terminate at some non-zero coupling, and hence not expected to cross. Extrapolated to normal regime, energies corresponding to different polarizations would be different, and also not cross. For a given g , E_g lies higher for smaller P , presumably due to the lower majority-species band becoming progressively more occupied with increasing P , thereby lowering E_g

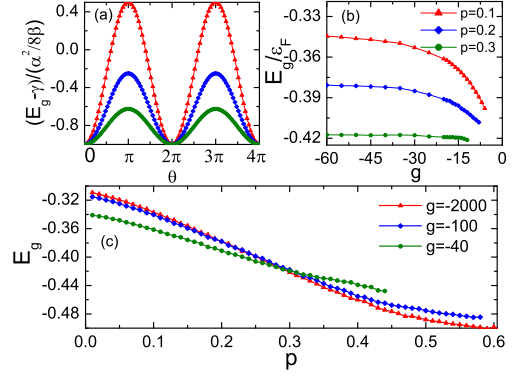


FIG. 3: (Color online) (a) Calculated ground state energy (scaled to global minimum) vs. relative phase angle θ (see text). Curve with maximal amplitude corresponds to state C in Fig 1: $|\Delta_0|^2 = -\alpha/8\beta$, $|\Delta_1|^2 = |\Delta_{-1}|^2 = -\alpha/16\beta$. Other two curves correspond to other representative states on the arc in Fig. 1: $|\Delta_0|^2 = -\alpha/11.3\beta$, $|\Delta_1|^2 = -\alpha/76.3\beta$, $|\Delta_{-1}|^2 = -\alpha/6.73\beta$; $|\Delta_0|^2 = -\alpha/16\beta$, $|\Delta_1|^2 = -\alpha/186\beta$, $|\Delta_{-1}|^2 = -\alpha/5.49\beta$. (b) Calculated ground state energy E_g vs. coupling g for different polarizations P . (c) Calculated E_g vs. P for different g .

with increasing polarization. For small P , E_g becomes less negative with increasing g . This trend is reversed for $P \geq 0.3$. The crossing at $P \approx 0.3$ is suggestive of a possible scaling using stretches in P and E_g .

Summary: With inter-species pairing interaction in a population-imbalanced Fermi system, we find a rich p-wave superfluid GS structure involving various sub-states of orbital angular momentum $\ell = 1$. States giving global and local energy minimum are associated with non-Morse and Morse critical points. The 3D geometric depiction adds insight into the superfluid states. Our numerical calculations suggest a quantum phase transition between two SF phases driven by polarization. Energies of a multitude of “mixed” SF states show oscillations with a relative phase angle, that could be observable in phase-sensitive experiments. Insight into the nature of the orbital part of our superfluid states may be gained from measuring angular dependence of momentum distributions; molecular spectroscopy using light radiation; or possibly zero sound attenuation. Our work should apply to other unequal-population Fermi systems, especially where p-wave intra-species couplings are small or negligible.

We acknowledge helpful discussions with Jason Ellis, Randy Hulet, Harry Kojima, and Adriana Moreo. The work was partly supported by funding from ICAM. One of us (F. Popescu) acknowledges an ICAM Fellowship.

-
- [1] Y. Maeno et al, Nature **372**, 532 (1994).
- [2] N S. Saxena, et al., Nature (London) **406**, 587 (2000); C. Pfleiderer et al., Nature **412**, 59 (2001); D.N. Aoki, et al., Nature (London) **413**, 613 (2001); N. T. Huy et al, Phys. Rev. Lett. **99**, 067006 (2007).
- [3] R. Casalbuoni and G. Nardulli, Rev. Mod. Phys. **76**, 263 (2004).
- [4] W. A. Coniglio et al, Phys. Rev. B **83**, 224507 (2011).
- [5] M. W. Zwierlein et al., Science **311**, 492 (2006); G. Partridge et al., Science **311**, 503 (2006); M. W. Zwierlein et al., Nature (London) **442**, 54 (2006); Y. Shin et al., Phys. Rev. Lett. **97**, 030401 (2006); G. Partridge et al., Phys. Rev. Lett. **97**, 190407 (2006); Y. Shin et al., Nature **451**, 689 (2008).
- [6] C.A. Regal et al., Phys. Rev. Lett. **92**, 040403 (2004); M. W. Zwierlein et al., Phys. Rev. Lett. **92**, 120403 (2004); C. Chin et al., Science **305**, 1128 (2004); T. Bourdel et al., Phys. Rev. Lett. **93**, 050402 (2004).
- [7] J. Zhang, et al., Phys. Rev. A **70**, 030702(R) (2004).
- [8] C.A. Regal, C. Ticknor, J.L. Bohn, and D.S. Jin, Phys. Rev. Lett. **90**, 053201 (2003).
- [9] C. Ticknor, C.A. Regal, D.S. Jin, and J.L. Bohn, Phys. Rev. A **69**, 042712 (2004).
- [10] C.H. Schunck, et al., Phys. Rev. A **71**, 045601 (2005).
- [11] Y. Nishida, arXiv:0810.1321 (2009)
- [12] Y. -J. Han et al, Phys. Rev. Lett. **103**, 070404 (2009)
- [13] C. Lai, C. Shi, S. -W. Tsa, arXiv:1206.6797 (2012).
- [14] V. Gurarie, L. Radzihovsky, A.V. Andreev, Phys. Rev. Lett. **94**, 230403 (2005).
- [15] C.-H. Cheng and S.-K. Yip, Phys. Rev. Lett. **95**, 070404 (2005).
- [16] S. S. Botelho, C.A.R. Sá de Melo, J. Low Temp. Phys. **140**, 409 (2005); M. Iskin and C.A.R. Sá de Melo, Phys. Rev. Lett. **96**, 040402 (2006).
- [17] Y. Ohashi, Phys. Rev. Lett. **94**, 050403 (2005).
- [18] Tin-Lun Ho and Roberto B. Diener, Phys. Rev. Lett. **94**, 090402 (2005).
- [19] A. Bulgac, M. Forbes, and A. Schwenk, Phys. Rev. Lett. **97**, 020402 (2006); Kelly R. Patton and D. E. Sheehy, Phys. Rev. A **83** 051607 (2011).
- [20] P. Fulde, and R. A. Ferrell, Phys. Rev. **135** A550 (1964); A. I. Larkin and Yu.N. Ovchinnikov, Zh. Eksp. Teor. Fiz. **47** 1136 (1964); A. I. Larkin and Yu.N. Ovchinnikov, Sov. Phys. JETP **20** 762 (1965);
- [21] H. Bruus and K. Flensberg, *Introduction to Many-body Quantum Theory in Condensed Matter Physics* (Oxford University Press Inc. New York, 2004).
- [22] R. Liao and K. Quader, Phys. Rev. B **76**, 212502 (2007).
- [23] $G_{\sigma,\sigma'} \equiv -\langle T_{\tau} c_{\mathbf{k}\sigma}(\tau) c_{\mathbf{k}\sigma'}^{\dagger}(0) \rangle$; $F_{\sigma,\sigma'} \equiv -\langle T_{\tau} c_{-\mathbf{k}\sigma}^{\dagger}(\tau) c_{\mathbf{k}\sigma}^{\dagger}(0) \rangle$. [21]
- [24] P. Nozières and S. Schmitt-Rink, J. of Low Temp. Phys. **59**, 195 (1985).
- [25] g is in terms of scattering parameters: triplet scattering volume a_t and effective range or equivalently cut-off momentum k_0 ; see M. Iskin and C.A.R. Sá de Melo, Phys. Rev. A **74**, 013608 (2006).
- [26] Reasoning similar to [18]. $\sum_{E_k > h} E_k = \sum_{|\Delta_k| > |\xi_k|} \sqrt{|\Delta_k|^2 + \xi_k^2} = \sum_{|\Delta_k| > |\xi_k|} \sqrt{|\Delta_k|^2 + |\xi_k|^2} + \sum_{|\Delta_k| \ll |\xi_k|} \sqrt{|\Delta_k|^2 + \xi_k^2} = \sum_{|\Delta_k| > h, |\xi_k| > h} |O(\Delta_k)| + \sum_{|\Delta_k| \ll |\xi_k|, \xi_k > h} \sqrt{|\Delta_k|^2 + \xi_k^2}$. 1st term negligible compared to 2nd: negligible integration domain; small integrand; $\sum_{E_k > h} E_k \simeq \sum_{|\Delta_k| \ll |\xi_k|, \xi_k > h} \sqrt{|\Delta_k|^2 + \xi_k^2}$; so, $\xi_k = 0$ excluded.
- [27] R. Gilmore, *Catastrophe Theory for Scientists and Engineers* (Dover Publications Inc., New York, 1993).
- [28] Based on Morse lemma and Thom's theorem/splitting lemma respectively for Morse and non-Morse critical points. $\det [H] = 0$ when one/more eigenvalues of Hessian, $H=0$. Thom's lemma can split H into blocks with non-zero determinants. [27]
- [29] Instability in stability matrix indicates instability to another phase, but not its nature. This is sufficient to map out phase boundary, e.g. critical polarization line P_c , where superfluid gap vanishes. Above P_c , system is in normal phase. Below P_c , stability of phases SF1 and SF2 are examined in turn to map out the phase diagram.